

Original Research Article

Developing a Decision Support Tool for Assessing Land Use Change and BMPs in Ungauged Watersheds Based on Decision Rules Provided by SWAT Simulation

Junyu Qi^{a*}, Sheng Li^{b,c}, Charles P.-A. Bourque^b, Zisheng Xing^{b,d}, and Fan-Rui Meng^b

^a Earth System Science Interdisciplinary Center, University of Maryland, College Park, 5825 University Research Ct, College Park, MD, 20740, USA

^b Faculty of Forestry and Environmental Management, University of New Brunswick, P.O. Box 44400, 28 Dineen Drive, Fredericton, NB, E3B 5A3, Canada

^c Potato Research Centre, Agriculture and Agri-Food Canada, P.O. Box 20280, 850 Lincoln Road, Fredericton, NB, E3B 4Z7, Canada

^d Portage La Prairie Site of Brandon Research and Development Centre, Agriculture and Agri-Food Canada, MB, Canada

***Corresponding author:** Junyu Qi, Tel.: +1 240 302 5689, E-mail: junyuqi@umd.edu

1 **Abstract**

2 Decision making on water resources management at ungauged, especially large-scale
3 watersheds relies on hydrological modeling. Physically-based distributed hydrological
4 models require complicated setup, calibration, and validation processes, which may delay
5 their acceptance among decision makers. This study presents an approach to develop a
6 simple decision support tool (DST) for decision makers and economists to evaluate multi-
7 year impacts of land use change and BMPs on water quantity and quality for ungauged
8 watersheds. The example DST developed in the present study was based on statistical
9 equations derived from Soil and Water Assessment Tool (SWAT) simulations applied to
10 a small experimental watershed in northwest New Brunswick. The DST was
11 subsequently tested against field measurements and SWAT simulations for a larger
12 watershed. Results from DST could reproduce both field data and model simulations of
13 annual stream discharge and sediment and nutrient loadings. The relative error of mean
14 annual discharge and sediment, nitrate-nitrogen, and soluble-phosphorus loadings were -6,
15 -52, 27, and -16%, respectively, for long-term simulation. Compared with SWAT, DST
16 has fewer input requirements and can be applied to multiple watersheds without
17 additional calibration. Also, scenario analyses with DST can be directly conducted for
18 different combinations of land use and BMPs without complex model setup procedures.
19 The approach in developing DST can be applied to other regions of the world because of
20 its flexible structure.

21 **Keywords:** multiple regression; hydrological model; erosion; nitrate leaching;
22 geographic information system

23

24 **1. Introduction**

25 Pollution from nonpoint sources poses a significant threat to ecosystems and plant and
26 animal communities (Vörösmarty et al., 2010). Nonpoint sources of sediment, nutrients,
27 and pesticides, primarily from agricultural lands, have been identified as major
28 contributors to water quality degradation (Zhang et al., 2004; Ongley et al., 2010). These
29 pollutants are difficult to control because they come from many sources (Quan and Yan,
30 2001). Practices such as strip cropping, terracing, crop rotation, and nutrient management
31 can be developed to prevent soil erosion and reduce the movement of nutrients and
32 pesticides from agricultural lands to aquatic ecosystems (D'Arcy and Frost, 2001). These
33 pollution-prevention methods, known as best management practices (BMPs), are
34 intended to minimize the negative environmental impact of agricultural activities, while
35 maintaining land productivity. Reliable information on the impacts of land use change
36 and BMPs on water quantity and quality is critical to watershed management
37 (Panagopoulos et al., 2011).

38 Many studies have been conducted to evaluate the impact of land use change and
39 BMPs on water quality based on field experiments (Novara et al., 2011; Pimentel and
40 Krummel, 1987; Sadeghi et al., 2012; Turkelboom et al., 1997; Urbonas, 1994). Monitoring
41 systems have been established to assess the impact of land use change and BMPs on
42 water resources in order to capture the spatial and temporal variation in soil, climate, and
43 topographic conditions in watersheds (Veldkamp and Lambin, 2001). Statistical models
44 developed from field data from small watersheds are usually assumed to apply to large
45 watersheds (Blöschl and Sivapalan, 1995; Blöschl and Grayson, 2001). Although it is not
46 difficult to quantify soil erosion and chemical loadings in experimental plots, it is time-

47 consuming and expensive (Mostaghimi et al., 1997). Clearly, it is not practical to conduct
48 field experiments for every possible combination of land use and BMPs, under different
49 biophysical conditions. As a result, it is unlikely sufficient field data could be obtained to
50 develop management plans and conduct cost-benefit analyses. In addition, statistical
51 models could be potentially derived from experiments; however, it is difficult to establish
52 cause-and-effect relationships between BMPs and water quality variables under varied
53 biophysical conditions or to quantify the impact of combined land use and BMPs on
54 water quality at the watershed scale (Renschler and Lee, 2005).

55 Process-based models of hydrology can be used to extrapolate field data to fill data
56 gaps (Borah and Bera, 2004;Borah and Bera, 2003;Singh, 1995;Singh and Woolhiser,
57 2002;Singh and Frevert, 2005). These process-based models provide quantitative
58 information that is usually difficult to obtain from field experiments (Borah et al., 2002).
59 For example, ANSWERS (Beasley et al., 1980), CREAMS (Knisel, 1980), GLEAMS
60 (Leonard et al., 1987), AGNPS (Young et al., 1989), EPIC (Sharpley and Williams,
61 1990), and SWAT (Arnold et al., 1998) have been used to understand surface runoff, soil
62 erosion, nutrient leaching, and pollutant-transport processes. However, these process-
63 based models require extensive input data and complex calibration procedures (Liu et al.,
64 2015); watersheds with sufficient data to calibrate and validate these models are normally
65 small, resulting in lack of representation at large spatial scales. Furthermore, once a
66 model is calibrated, parameters become watershed-specific, which cannot be easily
67 extended to other watersheds. In addition, these models require specialized expertise,
68 which prevents non-expert decision makers and economists to use them (Viavattene et al.,
69 2008).

70 A decision support tool could be developed by combining “decision rules” with
71 geographic information systems (GIS) for water quality assessment in large ungauged
72 watersheds. The “decision rules” could be based on regression equations derived from
73 field experiments (Renschler and Harbor, 2002), or they could be defined simply as
74 constants based on expert knowledge. Alternatively, simulations from a well-calibrated
75 hydrological model could be used to develop statistical equation-based “decision rules”.
76 Apart from defining “decision rules” at each grid cell, to assess water quantity and
77 quality in streams or at subbasin/watershed outlets, the decision support tool should
78 consider discharge, sediment, and nutrient routing within the watershed. For example, a
79 commonly used routing method for sediments is the sediment-delivery ratio (SDR)
80 method, which is widely employed in many GIS-based erosion models (May and Place,
81 2010;Wilson et al., 2001;Zhao et al., 2010). For discharge, a simple summation routing at
82 the outlet produces acceptable accuracy for small- and medium-sized watersheds,
83 considering that there is negligible water losses from surface runoff and stream flow. For
84 large watersheds, water losses are generally greater. These water losses can be estimated
85 using simple linear equations. The annual export of nutrients from watersheds (via the
86 nutrient-delivery ratio) has been studied empirically in many studies as nutrient loading
87 per land area (Endreny and Wood, 2003;Beaulac and Reckhow, 1982;Reckhow and
88 Simpson, 1980).

89 A decision support tool developed based on “decision rules” is generally flexible and
90 easy for decision makers and economists to use (Endreny and Wood, 2003). However,
91 their practicality in normal circumstances, particularly with respect to their level of
92 accuracy, needs to be evaluated. In addition, to provide sufficient “decision rules” with

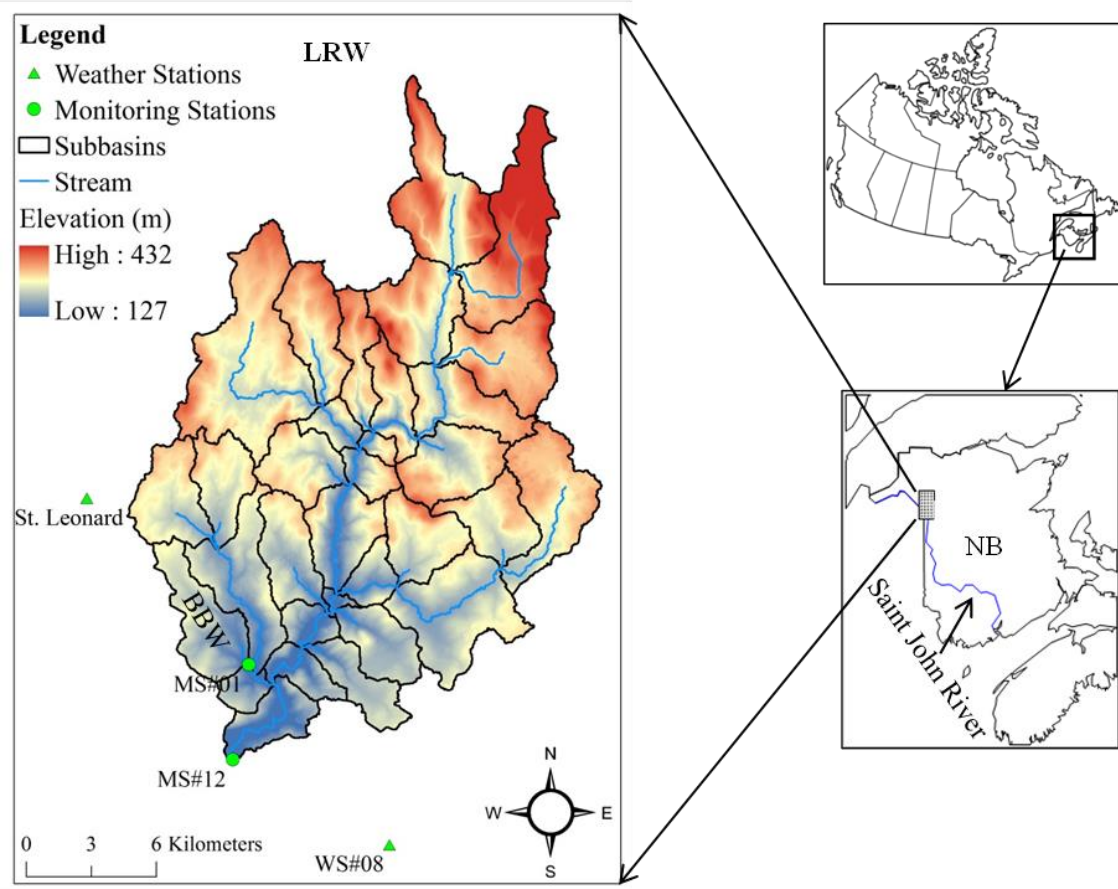
93 reasonable accuracy, fully validated hydrological models are required to be able to fill
94 data gaps in field experiments. The present study used the Soil and Water Assessment
95 Tool (SWAT) to provide modelled data in the development of the decision support tool.
96 The main objective of the present study is to develop a simple decision support tool with
97 the intent to evaluate the impact of land use change and BMPs on water resources in a
98 large ungauged watershed in New Brunswick, Canada. This paper presents the
99 development and testing of a decision support tool using data from two watersheds in the
100 potato-belt of New Brunswick; one small experimental watershed, with extensive
101 monitoring and field survey data, and a larger watershed containing the smaller
102 watershed. Specifically, this involves: (1) setting up, calibrating, and validating SWAT
103 for a small experimental watershed; (2) developing statistical equations relating water
104 quality and quantity variables with weather, soil, land use information based on SWAT
105 simulations for different combinations of land use and BMPs; (3) integrating the
106 statistical equations into a decision support tool with the aid of ArcGIS; and (4) testing
107 the decision support tool against field measurements and model simulations of stream
108 discharge, sediment, and nutrient loadings for a large watershed.

109 **2. Materials and Methods**

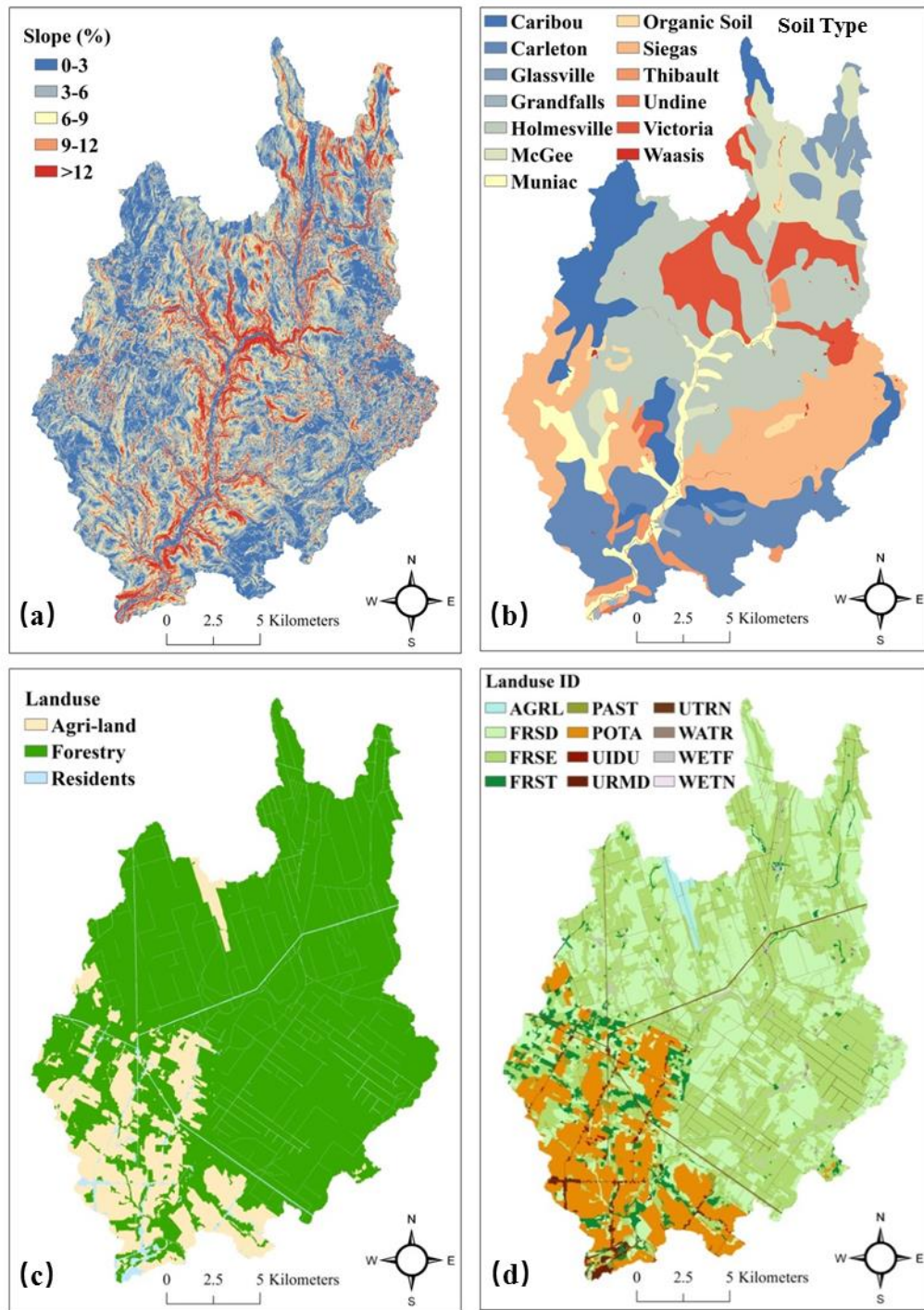
110 **2.1 Study Sites and Data Collection**

111 The large watershed of this study is the Little River Watershed (LRW), located in the
112 Upper Saint John River Valley of northwestern New Brunswick, Canada (Fig. 1). It
113 covers an area approximately 380 km² with a mixture of agricultural (16.2%), forest
114 (77%), and residential (6.8%) land uses (Xing et al., 2013). Elevation in the watershed
115 ranges from 127 to 432 m above mean sea level (Fig. 1). The soil in the study sites is

116 classified as mineral, derived from various parent materials. The major associations are
117 Caribou, Carleton, Glassville, Grandfalls, Holmesville, McGee, Muniac, Siegas, Thibault,
118 Undine, Victoria, Waasis, and one organic soil (Fig. 2). The study site belongs to the
119 Upper Saint John River Valley Ecoregion in the Atlantic Maritime Ecozone (Marshall et
120 al., 1999). The climate of the region is considered to be moderately cool boreal with
121 approximately 120 frost-free days, annually (Yang et al., 2009). Daily maximum and
122 minimum temperate are 24 (in July) and -18.1°C (in January) based on Canadian Climate
123 Normal station data at St. Leonard (http://climate.weather.gc.ca/climate_normals). The
124 average temperature is 3.7°C and annual precipitation is 1037.4 mm (Zhao et al., 2008).
125 About one-third of the precipitation is in the form of snow. Snowmelt leads to major
126 surface runoff and groundwater recharge events from March to May (Chow and Rees,
127 2006). The land use and soil maps in the setup of SWAT for LRW were derived from
128 publicly available data [Energy and Resource Development (ERD), New Brunswick; Fig.
129 2].



132 **Fig. 1** Location of the Little River Watershed (LRW) and Black Brook Watershed (BBW)
 133 in New Brunswick (NB), Canada and water-monitoring stations #01 and #12 as well as
 134 weather stations #08 and St. Leonard. Elevations and subbasins are also shown for LRW.



136

137 **Fig. 2** Slope classes created using a 10-m resolution LiDAR (Light Detection and
 138 Ranging)-based DEM (Digital Elevation Model), soil and land use maps, and land use
 139 IDs in SWAT (see Table 2 for land use ID meaning).

140 The small experimental watershed of the study is the Black Brook Watershed (BBW),
141 a subbasin of LRW (Fig. 1). The BBW has been studied extensively for more than 20
142 years to evaluate the impact of agriculture on soil erosion and water quality (Li et al.,
143 2014; Chow and Rees, 2006). The watershed covers an area of 14.5 km², with 65% being
144 agriculture land, 21% forest land, and 14% residential areas and wetlands. Slopes vary
145 from 1-6% in the upper basin to 4-9% in the central area. In the lower portion of the
146 watershed, slopes are more strongly rolling at 5-16%. Soil surveys (1:10,000 scale)
147 identified six mineral soils, namely Grandfalls, Holmesville, Interval, Muniac, Siegas,
148 and Undine, and one organic soil, St. Quentin (Mellerowicz, 1993).

149 A water-monitoring station was established at the outlet of BBW in 1992 (MS#01; Fig.
150 1) and another (MS#12) at the outlet of LRW in 2001. At these stations, V-notch weirs
151 were installed, and the stage height of the water was recorded using a Campbell-
152 Scientific CR10X data logger. Stage height values were converted to total flow rates with
153 a calibration curve function (Chow et al., 2011). Water samples were collected with an
154 ISCO automatic sampler. Sampling frequency was set at one sample every 72 hours when
155 runoff was absent. During runoff events, sampling frequency was increased to one
156 sample every 5-cm change in stage height. Samples were analyzed for concentration of
157 suspended solids, nitrate-nitrogen (NO₃-N), and soluble-phosphorus (Sol-P). Detailed
158 description of data collection procedures and sample analyses can be found in Chow et al.
159 (2011). Weather data including daily precipitation, air temperature, relative humidity, and
160 wind speed were acquired from the St. Leonard Environment Canada weather station
161 (<http://climate.weather.gc.ca>), located approximately 5 km northwest of BBW (Fig. 1).
162 The daily average relative humidity and wind speed were calculated based on averaging

163 hourly values. Since this weather station did not monitor daily solar radiation, the study
164 used solar radiation collected from a weather station located approximately 10 km
165 southeast of BBW (WS#08; Fig. 1).

166 **2.2 SWAT Setup, Calibration, and Validation for BBW and LRW**

167 A modified version of SWAT has been developed for cold regions (Qi et al.,
168 2017a;Qi et al., 2016a, b;Qi et al., 2017b), and it was used for the BBW and LRW in this
169 study. Detailed model setup, calibration, and validation for BBW can be found in Qi et al.
170 (2017b). Specific model inputs for both watersheds are provided in Table 1. The same
171 weather data were used for both watersheds (Table 1). The Digital Elevation Model
172 (DEM) for LRW and BBW were both based on high resolution LiDAR (Light Detection
173 and Ranging) data, the first was created at 10-m and the second, at 1-m resolution. The
174 LRW was delineated into 32 subbasins from which their topographic characteristics were
175 defined (Fig. 1). The soil types and slopes, which were classified into five separate
176 classes, are illustrated in Fig. 2 for LRW. After combining the soil, slope, and land use
177 maps through the ArcSWAT-interface function, 362 HRUs were subsequently created for
178 LRW (based on thresholds: 10, 15, and 20% for land use, soil, and slope).

179

180

181

182

183

184

185

186 **Table 1** Datasets in SWAT setup, calibration, and validation for BBW and LRW.

Dataset	BBW	LRW
LiDAR DEM resolution	1-m	10-m
Soil map	Survey (1993)	ERD
Land use maps	Survey (1992-2011)	ERD (one map)
Precipitation, temperature, relative humidity & wind speed	St. Leonard (1992-2011)	St. Leonard (2001-2010)
Solar radiation	WS#08 (1992-2011)	WS#08 (2001-2010)
Contour tillage operation (spring and fall)	Survey (1992-2011)	Only for potato and barley (2001-2010)
Fertilizer application	Survey (1992-2011)	Estimated from BBW (2001)
Crop rotation	Survey (1992-2011)	Potato-barley (2001-2010)
Terraces and grassed waterways	Survey (1992-2011)	Negligible
Discharge, sediment, $\text{NO}_3\text{-N}$ and Sol-P	MS#01 (1992-2011)	MS#12 (2001-2010)

187

188 Since only one land use map was available for LRW (Table 1), assumptions were
 189 made based on information available on land use and management records for BBW to
 190 adjust the SWAT-management files for LRW as follows:

191 (1) Potato-barley rotations were assigned to the land use ID POTA (Table 2); for other
 192 land use IDs, a single crop was considered;

193 (2) Fertilizers were applied only to potato and barley fields, and fertilizer amounts and
 194 N:P (nitrogen-to-phosphorus) ratios were averaged for potato and barley fields over the
 195 entire watershed, based on 2001 survey data from BBW;

196 (3) Contour tillage was applied only to potato and barley fields;

197 (4) Flow diversion terraces (FDT) and grassed waterways in LRW were assumed not
 198 used. It is worth noting that these four assumptions serve as a baseline scenario for the
 199 assessment of FDT in LRW.

200 To evaluate the global performance of the decision support tool for LRW, related
 201 land use and management files were prepared and accessed by SWAT. For purpose of

202 comparison, simulations with SWAT were produced in an initial application by setting
203 the adjustable parameters of the model to their default values, and in a second application
204 by setting the parameters according to values produced with a watershed-specific model
205 calibration to BBW. This approach with model parameterization is widely accepted when
206 applying SWAT to large ungauged watersheds (Panagopoulos et al., 2011).

207 **2.3 Decision Rules**

208 The decision support tool was designed to use the “decision rules” to estimate annual
209 discharge and sediment and nutrient loadings from individual grid cells:

210
$$A = \sum_{i=1}^n DR_i \cdot A_i, \quad (1)$$

211 where A is the annual discharge or sediment and nutrient loadings at the outlet of the
212 watershed, DR_i and A_i are the delivery ratios and annual discharge or loadings,
213 respectively, for grid cell i . For the present study, statistical equations derived from
214 simulations of the calibrated version of SWAT for BBW were defined as the “decision
215 rules” in the decision support tool.

216 **2.3.1 Land Use Groups and BMP Scenarios**

217 In statistical equation development, land use in BBW (24, in total) was first classified
218 into five land use classes according to their influences on hydrological processes (Table
219 2). Note that WATR was not used due to its small overall coverage (Fig. 2). As for
220 watershed management, we considered three main BMPs, i.e.,

221 (1) FDT + contour tillage;
222 (2) Contour tillage; and
223 (3) No-BMP (without FDT and contour tillage).

224

225

Table 2 Land use and land use groups (LUGP) for BBW and LRW.

LUGP	Land use ID in SWAT	Land use type
AGRL (General crops)	AGRL	Agricultural Land-Generic
	CANA	Canola
	CRON	Corn
	FPEA	Field peas
	POTA	Potato
GRAN (Grains)	BARL	Barley
	OATS	Oats
	PMIL	Millet
	RYE	Rye
	SWHT	Spring wheat
GRAS (Grasses)	WWHT	Winter wheat
	BERM	Bermuda grass
	CLVR	Clover
	HAY	Hay
	PAST	Past
FORT (Forestry)	RYEG	Ryegrass
	TIMO	Timothy
	FRSD	Forest-Deciduous
	FRSE	Forest-Evergreen
	FRST	Forest-Mixed
NOCR (Non-vegetated lands)	RNGB	Range-Bush
	WETF	Wetlands-Forested
	WETN*	Wetlands-No-Forest
	URMD	Residential
	UTRN	Transportation
	UIDU*	Industrial

Note: “*” indicates unique land use types to LRW not present in BBW and, therefore, unaccounted for in the development of the decision support tool.

226

227 The calibrated version of the enhanced SWAT for BBW was used to generate annual
 228 outputs based on HRUs from 1992 to 2011. The model was run three times to generate
 229 the BMP-specific data for statistical equation development.

230

231 2.3.2 Explanatory Variables Selection

232 Explanatory candidate variables must be physically-meaningful in hydrological and
233 biochemical processes. It is worth noting that both continuous and categorical variables
234 were included in the regression equation. The land use group (LUGP) was the only
235 categorical variable, and the remaining were all continuous variables. To detect
236 significant predictors, the analysis of covariance (ANCOVA) was used. It requires at
237 least one continuous and one categorical explanatory variable and is used to identify the
238 major and interaction of predictor variables. By including continuous variables, the
239 method can reduce the variance of error to increase the statistical power and precision in
240 estimating categorical variables (Keselman et al., 1998; Li et al., 2014). Inclusion of
241 interaction terms in these regression models dramatically increased model performance.

242 In the present study, we only considered interactions between two explanatory variables
243 at a time. Student t-tests were conducted to examine the statistical significance of each
244 level of LUGP and their interaction with the various continuous variables. When one
245 level of LUGP (e.g., GRAN; Table 2) did not significantly correlate with water quality or
246 quantity, or there were nominal interactions between a given level and other explanatory
247 variables, this particular level of LUGP would be combined with other levels of LUGP
248 until all new levels of LUGP were statistically significant.

249 Multiple linear regression analyses were used to relate annual total discharge (mm) and
250 sediment ($t\ ha^{-1}$), NO_3-N ($kg\ ha^{-1}$), and $Sol-P$ ($kg\ ha^{-1}$) loadings to the explanatory
251 variables. These work was conducted in R (Ihaka and Gentleman, 1996). Only six
252 continuous explanatory variables were determined for the specification of the statistical
253 models. Annual precipitation (PCP), annual mean air temperature (TMP), and mean
254 saturated hydraulic conductivity of soil (SOL_K) were common to the dependent

255 variables (i.e., total discharge and sediment, $\text{NO}_3\text{-N}$, and Sol-P loadings). The LS-factor
256 (USLE_LS) and annual N and P application rates (N_APP and P_APP) were unique to
257 the equations addressing sediment, $\text{NO}_3\text{-N}$, and Sol-P loading.

258 **2.3.3 Delivery Ratio Definition**

259 The LS-factor of the universal soil loss equation (USLE) was determined by slope
260 gradient (slp) and slope length (L) of individual HRUs:

261
$$\text{USLE_LS} = \left\{ \frac{L}{22.1} \right\}^m \cdot (65.41 \cdot \sin^2(a) + 4.56 \cdot \sin(a) + 0.065) \quad (2)$$

262 where m is the equation exponent and a is the angle of the slope (in degrees). The
263 exponent m is calculated by,

264
$$m = 0.6 \cdot (1 - \exp[-35.835 \cdot slp]) \quad (3)$$

265 where slp is in units of m m^{-1} . For the decision support tool, slope length L equals to the
266 length of the grid side and slope gradient was determined by the *Slope* tool in ArcGIS.
267 The sediment-delivery ratio was not considered in the decision support tool application to
268 BBW. We assumed that annual sediment loadings from grid cells in decision support tool
269 were all exported to the outlet of BBW. However, when the decision support tool was
270 applied to LRW, the sediment-delivery ratio was used to correct estimates of sediment
271 loading at the watershed outlet. The sediment loadings at the outlet of LRW (sed) were
272 determined by

273
$$sed = SDR \cdot sed^{\sim} \quad (4)$$

274 where sed^{\sim} is the sediment loading calculated with the sediment loading equation (one for
275 each BMP and land use group), and SDR is determined by (Vanoni, 1975)

276
$$SDR = 0.37 \cdot D^{-0.125} \quad (5)$$

277 where D (km^{-2}) is the drainage area. For annual discharge and nutrient loadings, we
278 assumed their delivery ratios equal to 1.0 for all grid cells in LRW.

279 **2.4 Decision Support Tool Assessment**

280 Inputs to the decision support tool included the six continuous explanatory variables
281 and LUGP as well as information on management practices, e.g., contour tillage and FDT
282 implementation. Simulations from each grid cells were summarized at the outlet of the
283 study watersheds. We first tested the impact of cell size on simulations of water quantity
284 and quality at the outlet of BBW. The cell size range was determined by considering
285 different farmland sizes in the watershed. We assumed that farmland-based grid cells can
286 sufficiently represent basic hydrological processes, land use change, and management
287 practice implementations for hydrological modeling. Simulated annual water flow and
288 sediment and nutrient loadings with the decision support tool were compared with those
289 produced with the calibrated version of the enhanced SWAT. Subsequently, the decision
290 support tool was applied to LRW, and the simulations were compared with the results of
291 the uncalibrated and calibrated versions of SWAT. The purpose of this was to test if the
292 decision support tool (i.e., land use and BMP assessment tool; LBAT) performed better,
293 or at least as well, as both the uncalibrated and calibrated version of SWAT.

294 Model performance in terms of water quantity and quality at the outlet of the study
295 watersheds was assessed based on the coefficient of determination (R^2) and relative error
296 (Re), i.e.,

$$297 R^2 = \left(\frac{\sum_{i=1}^n (o_i - o_{avg}) \cdot (p_i - p_{avg})}{\left[\sum_{i=1}^n (o_i - o_{avg})^2 \cdot \sum_{i=1}^n (p_i - p_{avg})^2 \right]^{0.5}} \right)^2 \quad (6)$$

$$298 Re = \frac{(p_{avg} - o_{avg})}{o_{avg}} \cdot 100\% \quad (7)$$

299 where O_i , P_i , O_{avg} , and P_{avg} are the observed and predicted and averages of the observed
300 and predicted values, respectively.

301

302 **2.5 FDT Assessment in LRW**

303 A series of FDT-implementation scenarios were set up for LBAT based on six slope
304 classes to assess the impact of FDT on water quantity and quality on agricultural lands in
305 LRW (Fig. 3; Table 3). From scenarios one (S1) to six (S6), total area protected by FDT
306 gradually increased until all agricultural lands were protected (Table 3). Mean annual
307 simulations of total discharge and sediment, NO_3-N , and Sol-P loadings from LRW from
308 2001 to 2010 were compared with those of the baseline scenario (FDT = 0%) for each
309 scenario using two performance indicators, i.e., mean difference (MD) and % relative
310 difference (PRD), given as:

311 (1) $MD = \text{output with FDT} - \text{output without FDT}$, and

312 (2) $PRD (\%) = \frac{MD}{\text{output without FDT}} \times 100$.

313

314 **Table 3** Slope classes and corresponding areas in the agricultural land of LRW.

Scenario	Slope	Area protected by FDT (ha)	Agricultural lands (%)
S1	$\geq 5\%$	624	10
S2	$\geq 4\%$	1328	22
S3	$\geq 3\%$	2224	37
S4	$\geq 2\%$	3680	61
S5	$\geq 1\%$	5360	89
S6	≥ 0	6048	100

315

316

317 **3. Results and Discussion**

318 **3.1 Statistical Equations (Decision Rules)**

319 **3.1.1 Model Structure and Coefficients**

320 Linear regression equations and their explanatory variables for annual discharge and
321 sediment, $\text{NO}_3\text{-N}$, and Sol-P loadings under different combinations of land use groups
322 and BMP scenarios are provided in Tables 4 and 5. In total, three discharge models (Dis1,
323 Dis2, and Dis3) and five sediment (Sed1_1, Sed1_2, Sed1_3, Sed2, and Sed3), $\text{NO}_3\text{-N}$
324 (N1_1 , N1_2 , N1_3 , N2 , and N3), and Sol-P (P1_1 , P1_2 , P1_3 , P2 , and P3) loading
325 models were developed. Data transformations (via logarithm and power transformations)
326 were applied to sediment, $\text{NO}_3\text{-N}$, and Sol-P loadings to meet the assumption of
327 normality in multiple regression analysis (Table 4). The contour tillage and FDT were
328 applied only to agricultural lands, including land use groups AGRL, GRAN, and GRAS
329 (Table 4). For the no-BMP scenario, three separate sediment, $\text{NO}_3\text{-N}$, and Sol-P loading
330 models were developed for agricultural lands (AGRL, GRAN, and GRAS), non-
331 vegetated lands (NOCR), and forest lands (FORT), and one discharge model (Dis1) for
332 all land use groups (Table 4). It is worth noting that the sediment loading model, Sed3,
333 was a modified version of Sed1_1 (multiplied by TERR_P) for the FDT + contour tillage
334 scenario (Table 4), and the values of TERR_P (Qi et al., 2017b) used for Sed3 were the
335 same as the calibrated values in SWAT for BBW (Qi et al., 2017b). Also, $\text{NO}_3\text{-N}$ and
336 Sol-P loadings (N1_2 and P1_2) for non-vegetated lands (NOCR) were determined as
337 constants, which were equal to the calculated means of $\text{NO}_3\text{-N}$ and Sol-P loadings
338 determined by SWAT (i.e., 24 and 0.61 kg ha^{-1} , respectively; Table 4).

339 As for LUGP (including AGRL, GRAN, GRAS, FORT, and NOCR; Table 2), three
340 new land use groups (i.e., LUGP1, LUGP2, and LUGP3) were formulated by combining
341 agricultural lands AGRL, GRAN, and GRAS during model development (Tables 4 and 5).
342 For example, LUGP2 was derived by combining AGRL, GRAN, and GRAS on total
343 discharge (i.e., Dis1 model). Individual model structures are shown in Table 4, whereas
344 the explanatory variables for these models appear in **Appendix A**. The coefficients
345 estimated for the explanatory variables and their interactions, and their t-test results are
346 also shown in **Appendix A**. Most of the *p*-values for these explanatory variables were <
347 0.001, except for several that were between 0.001 and 0.08, which were also taken as
348 acceptable.

349

350

351

352

Table 4 Statistical models based on land use groups (LUGP) and BMPs.

BMPs	LUGP*	Model	Structure
No-BMP	CRGP2, NOCR, FORT	Dis1	Discharge = $f(\text{PCP}, \text{TMP}, \text{SOL_K}, \text{LUGP2})$
Contour tillage	AGRL, GRAN, GRAS	Dis2	= $f(\text{PCP}, \text{TMP}, \text{SOL_K})$
FDT+Contour tillage	AGRL, GRAN, GRAS	Dis3	= $f(\text{PCP}, \text{TMP}, \text{SOL_K})$
No-BMP	CRGP1, GRAS	Sed1_1	Sediment ^(1/10) = $f(\text{USLE_LS}, \text{PCP}, \text{TMP}, \text{SOL_K}, \text{LUGP1})$
	NOCR	Sed1_2	= $f(\text{USLE_LS}, \text{PCP})$
	FORT	Sed1_3	= $f(\text{USLE_LS}, \text{PCP}, \text{SOL_K})$
Contour tillage	CRGP1, GRAS	Sed2	Sediment ^(1/10) = $f(\text{USLE_LS}, \text{PCP}, \text{TMP}, \text{SOL_K}, \text{LUGP1})$
FDT+Contour tillage	AGRL, GRAN, GRAS	Sed3	Sediment = Sed1_1 × TERR_P
No-BMP	AGRL, GRAN, GRAS	N1_1	$\text{Log}(\text{NO}_3\text{-N}) = f(\text{N_APP}, \text{PCP}, \text{TMP}, \text{SOL_K}, \text{LUGP})$
	NOCR	N1_2**	$\text{NO}_3\text{-N} = 24 \text{ kg ha}^{-1}$
	FORT	N1_3	$\text{Log}(\text{NO}_3\text{-N}) = f(\text{PCP}, \text{TMP}, \text{SOL_K})$
Contour tillage	AGRL, GRAN, GRAS	N2	$\text{Log}(\text{NO}_3\text{-N}) = f(\text{N_APP}, \text{PCP}, \text{TMP}, \text{SOL_K}, \text{LUGP})$
FDT+Contour tillage	CRGP3, GRAN	N3	= $f(\text{N_APP}, \text{PCP}, \text{TMP}, \text{SOL_K}, \text{LUGP3})$
No-BMP	CRGP1, GRAS	P1_1	$\text{Log}(\text{Sol-P}) = f(\text{P_APP}, \text{PCP}, \text{TMP}, \text{SOL_K}, \text{LUGP1})$
	NOCR	P1_2**	$\text{Sol-P} = 0.61 \text{ kg ha}^{-1}$
	FORT	P1_3	$\text{Log}(\text{Sol-P}) = f(\text{PCP}, \text{TMP}, \text{SOL_K})$
Contour tillage	CRGP1, GRAS	P2	$\text{Log}(\text{Sol-P}) = f(\text{P_APP}, \text{PCP}, \text{TMP}, \text{SOL_K}, \text{LUGP1})$
FDT+Contour tillage	AGRL, GRAN, GRAS	P3	= $f(\text{P_APP}, \text{PCP}, \text{TMP}, \text{SOL_K}, \text{LUGP})$

353 *AGRL and GRAN are combined into one group, namely CRGP1 in LUGP1; AGRL, GRAN and GRAS are combined into one group, namely

354 CRGP2 in LUGP2; AGRL and GRAS are combined into one group, namely CRGP3 in LUGP3; ** variable is set constant.

21

355

Table 5 Explanatory variables determined for statistical analysis.

Variable	Unit	Meaning
LUGP	—	Land use groups including AGR, GRAN, GRAS, FORT, and NOCR
LUGP1	—	AGR and GRAN are combined into a new group, CRGP1
LUGP2	—	AGR, GRAN, and GRAS are combined into a new group, CRGP2
LUGP3	—	AGR and GRAS are combined into a new group, CRGP3
N_APP	kg ha ⁻¹	Annual N application rate
P_APP	kg ha ⁻¹	Annual P application rate
PCP	mm	Annual precipitation
SOL_K	mm h ⁻¹	Mean saturated hydraulic conductivity of soil
TERR_P	—	P-factor for FDT
TMP	°C	Annual mean air temperature
USLE_LS	—	LS-factor of USLE

356

357 **3.1.2 Statistical Equation Assessment**

358 Simulations based on the statistical equations and the calculated outputs from
 359 individual HRUs for the different BMPs are compared in Table 6. In general, discharge
 360 models were able to reproduce SWAT simulations for the three BMPs; R^2 ranging from
 361 0.86 to 0.9. Mean discharge simulated with the statistical equations was equal to that of
 362 SWAT (Table 6). Mean discharge (636 mm) for the no-BMP-case (BMP 3) was greater
 363 than that for BMPs using contour tillage and FDTs (619 and 628 mm for BMP 1 and 2,
 364 respectively), suggesting that contour tillage and FDTs can cause evapotranspiration to
 365 increase.

366 Models Sed1_2 and Sed1_3 were able to reproduce simulations with SWAT (yielding
 367 $R^2 = 0.71$ and 0.57, respectively), and simulated mean sediment loadings were close to
 368 that of SWAT (Table 6). Models Sed1_1 and Sed2 tended to underestimate results from
 369 SWAT (Table 6), with an overall lower mean sediment loading of 10.78 vs. 12.84 and
 370 8.31 vs. 9.4 t ha⁻¹, respectively. Mean sediment loading with Sed3 (0.89 t ha⁻¹) was
 371 slightly greater than that of SWAT (0.84 t ha⁻¹), because Sed3 only took into account

372 TERR_P, whereas SWAT took into account TERR_CN and the impact of grassed
373 waterways. Results from the statistical equations showed that the mean sediment loading
374 for BMP 2 (8.31 t ha^{-1}) was significantly different than that for BMPs 1 and 3, with mean
375 loading of 0.89 and 10.78 t ha^{-1} (Table 6). The smallest mean sediment loading (0.09 t ha^{-1})
376 was found to occur with the FORT land use grouping (Table 6).

377 The four $\text{NO}_3\text{-N}$ and Sol-P loading equations explained ~50% of the variation in the
378 SWAT simulations for the same variables, with R^2 ranging from 0.33 to 0.59 (Table 6).
379 Mean $\text{NO}_3\text{-N}$ and Sol-P loadings with the statistical equations were all slightly less than
380 the values produced with SWAT for the different BMPs (Table 6). Mean $\text{NO}_3\text{-N}$ loadings
381 were greater for BMP 1 (44 kg ha^{-1}) than those for BMPs 2 and 3 with both giving 39 kg
382 ha^{-1} (Table 6), due to increased infiltration with FDT. Mean Sol-P loading (0.8 kg ha^{-1})
383 was less for BMP 3 than for BMP 2 (0.89 kg ha^{-1}), whereas much greater than for BMP 1
384 (0.43 kg ha^{-1}). Although contour tillage can help reduce sediment loading by modifying
385 micro-topography and reducing erosion runoff (the reason we set USLE_P < 1), Sol-P
386 transported with surface runoff increased due to reduced residue cover protecting the soil
387 surface during winter and during the snowmelt season. When FDT was implemented with
388 tillage, however, less surface runoff was generated due to increased infiltration leading to
389 a reduction in Sol-P loading. Mean $\text{NO}_3\text{-N}$ and Sol-P loadings for the FORT land
390 grouping ($10 \text{ vs. } 0.06 \text{ kg ha}^{-1}$) were much less than those of the CRGP land grouping, 39
391 vs. 0.8 kg ha^{-1} (Table 6).

392 **Table 6** Comparisons of simulations of statistical models and outputs from SWAT for different land use groups and BMPs based on
 393 mean and standard deviation for the entire simulation period (1992-2011).

Variable	Index	No-BMP				Tillage		FDT + Tillage	
		CRGP		NOCR		FORT		CRGP	
		SWAT	Fitted	SWAT	Fitted	SWAT	Fitted	SWAT	Fitted
Discharge (mm)	Mean	→	→	636	636	←	←	619	619
	SD	→	→	144	133	←	←	140	132
	R ²	→	→	0.86 (Dis1)		←	←	0.88 (Dis2)	0.90 (Dis3)
Sediment (t ha ⁻¹)	Mean	12.84	10.78	1.80	1.71	0.10	0.09	9.40	8.31
	SD	11.86	9.44	1.94	1.95	0.14	0.16	8.28	7.38
	R ²	0.48 (Sed1_1)		0.71 (Sed1_2)		0.57 (Sed1_3)		0.56 (Sed2)	
NO ₃ -N (kg ha ⁻¹)	Mean	43	39	24	—	10	10	43	39
	SD	24	14	16	—	6	3	24	14
	R ²	0.40 (N1_1)		—		0.33 (N1_3)		0.39 (N2)	
Sol-P (kg ha ⁻¹)	Mean	0.88	0.80	0.61	—	0.08	0.06	0.98	0.89
	SD	0.49	0.32	0.46	—	0.06	0.03	0.59	0.38
	R ²	0.47 (P1_1)		—		0.38 (P1_3)		0.48 (P2)	

24 Note: CRGP refers to crop groups including AGRL, GRAN, and GRAS; the statistics for discharge in no-BMP scenario are

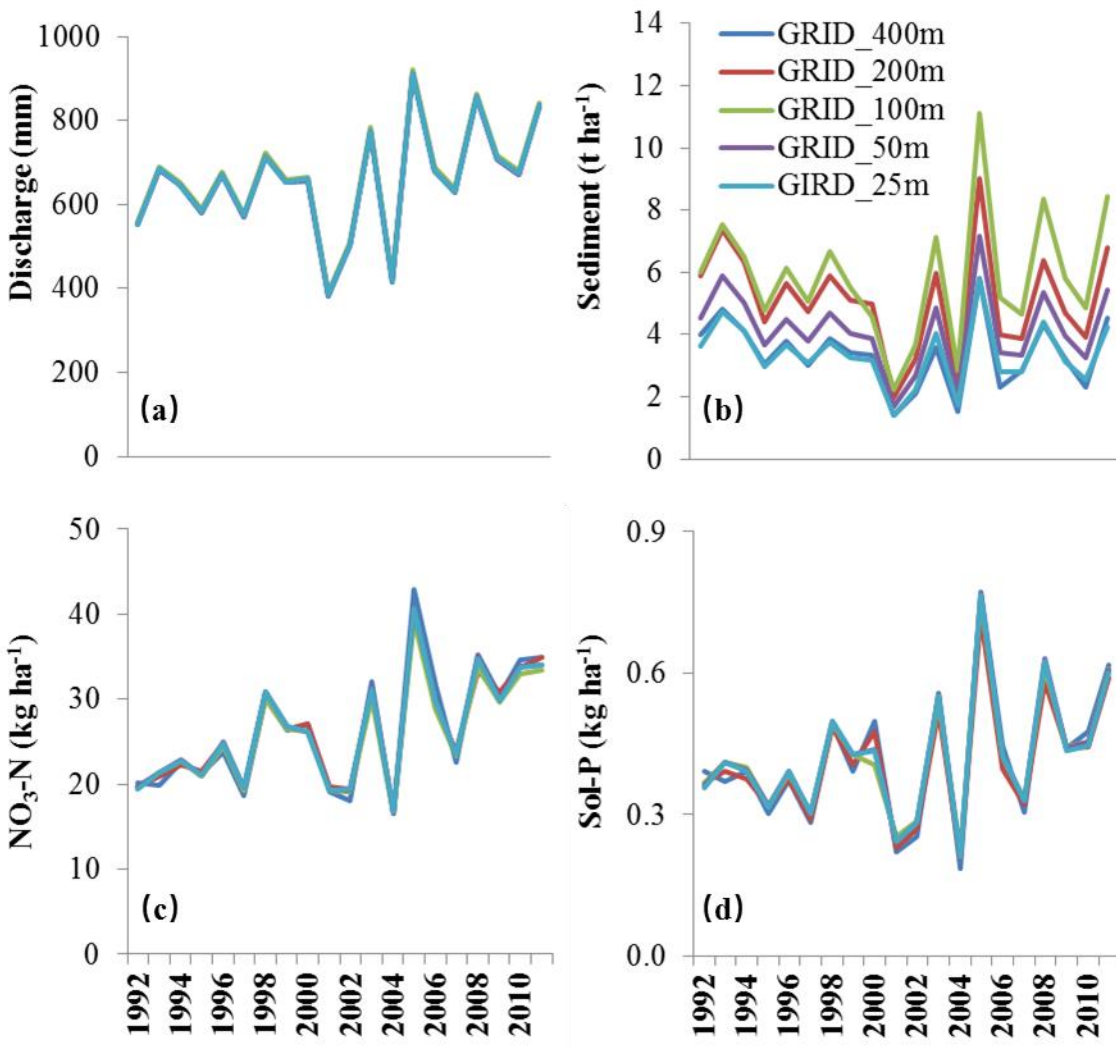
394

395 based on CRGP, NOCR, and FORT.

396 **3.2 LBAT Assessment**

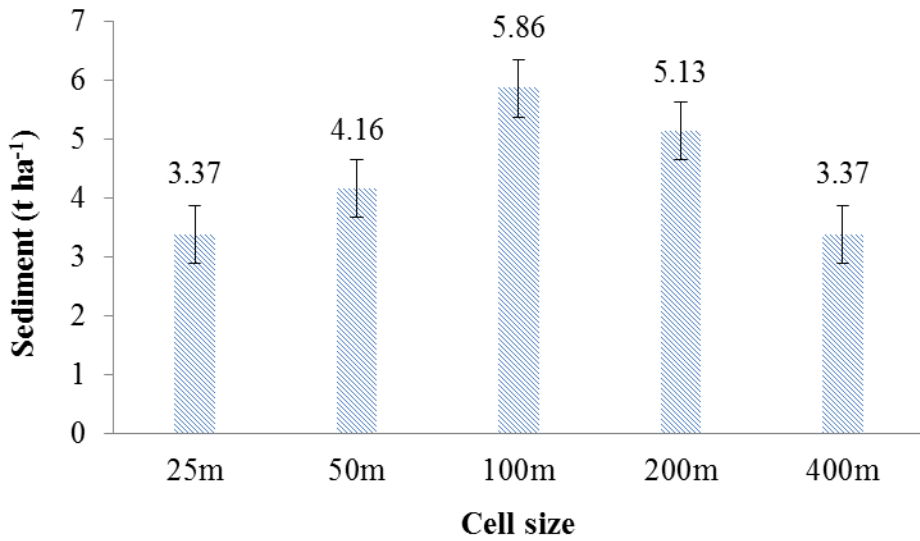
397 **3.2.1 Impact of Grid Cell Size on LBAT Simulation**

398 Simulations of water quantity and quality by LBAT with different grid-cell sizes (i.e.,
399 25, 50, 100, 200, and 400 m) for BBW are shown in Fig. 3. Statistical tests indicated that
400 grid-cell size had a significant effect on sediment loading (p -value < 0.01), with no effect
401 observed for discharge and $\text{NO}_3\text{-N}$ and Sol-P loadings (p -values > 0.99). Increasing cell
402 size (i.e., slope length) increased sediment loading. However, the mean slope gradient
403 was reduced. As a result, the mean sediment loadings were correlated non-linearly with
404 cell size as shown in Fig. 4. The highest mean sediment loading was found with a cell
405 size of 100 m (5.86 t ha^{-1}), whereas the lowest was found to occur with a cell size of 25
406 and 400 m (3.37 t ha^{-1}). The LBAT with a cell size of 25 and 400 m was able to generate
407 sediment loadings consistent with field measurements. Considering computational
408 efficiency, we chose a grid-cell size of 400 m as the basic LBAT-simulation unit for
409 LRW.



410

411 **Fig. 3** LBAT-produced simulations of annual stream discharge and sediment, NO₃-N, and
 412 Sol-P loadings determined for different DEM grid-cell sizes (i.e., 25, 50, 100, 200, and
 413 400 m).



414

415 **Fig. 4** Impact of grid-cell size on LBAT-simulation of sediment loading. Mean annual
416 sediment loadings and standard errors (vertical bars) from 1992 to 2011 are indicated.

417 **3.2.2 LBAT vs. SWAT in LRW**

418 Simulations of water quantity and quality with LBAT and the uncalibrated and
419 calibrated versions of SWAT are compared with field measurements for LRW (Fig. 5).
420 Model assessments for different simulation periods (depending on measurement
421 availability) are shown in Table 7. It is worth noting that, to eliminate unrealistic results,
422 USLE_LS was constrained in Sed1_2 to the NOCR land use group:

423
$$\text{USLE_LS} = \begin{cases} \text{Eq. 6-1} & \text{USLE_LS} \leq 1.28 \\ 1.28 & \text{USLE_LS} > 1.28 \end{cases} \quad (8)$$

424 where 1.28 is the maximum USLE_LS for BBW.

425 In general, the two versions of SWAT and LBAT slightly underestimated annual
426 stream discharge, capturing its variation reasonably well ($R^2 > 0.54$; Fig. 5a). The
427 uncalibrated and calibrated versions of SWAT had the least and largest absolute values of
428 Re ($Re = -2$ and -9), whereas LBAT $Re = -6$ (Table 7). The uncalibrated version of
429 SWAT severely overestimated annual sediment and $\text{NO}_3\text{-N}$ loading ($Re = 212$ and 87 ,
430 respectively; Figs. 5b and c), whereas the calibrated version of SWAT and LBAT
431 underestimated sediment loading ($Re = -32$ and -52 , respectively) and overestimated
432 $\text{NO}_3\text{-N}$ loading ($Re = 22$ and 27 , respectively; Table 7). In general, the calibrated version
433 of SWAT and LBAT captured the variation in annual $\text{NO}_3\text{-N}$ loadings reasonably well
434 ($R^2 > 0.35$; Fig. 5c). However, the two versions of SWAT and LBAT failed to capture the
435 variation in annual sediment and Sol-P loadings (low R^2 ; Figs. 5b and d). The LBAT had
436 the smallest absolute value of Re (i.e., $Re = -16$), while the uncalibrated and calibrated
437 versions of SWAT had larger values ($Re = -59$ and -55 , respectively). These results
438 suggested that the LBAT and the calibrated version of SWAT performed fairly
439 equivalently in simulating annual stream flow and sediment and $\text{NO}_3\text{-N}$ loadings, with

440 LBAT performing slightly better for annual Sol-P loading. LBAT performed noticeably
 441 better than the uncalibrated version of SWAT, especially for annual sediment and NO₃-N
 442 loadings. Poor performance for both versions of SWAT and LBAT on simulation of
 443 annual sediment and Sol-P loadings in LRW might attribute to lack of detailed
 444 management practice and fertilizer application information from agricultural lands. We
 445 only had one-year data for LRW and made assumptions about rotation and management
 446 practices for other years based on information from BBW, which could introduce major
 447 input uncertainty.

448

449 **Table 7** Statistical assessments of LBAT and SWAT for annual stream discharge and
 450 sediment, NO₃-N, and Sol-P loadings at the outlet of LRW for different simulation
 451 periods

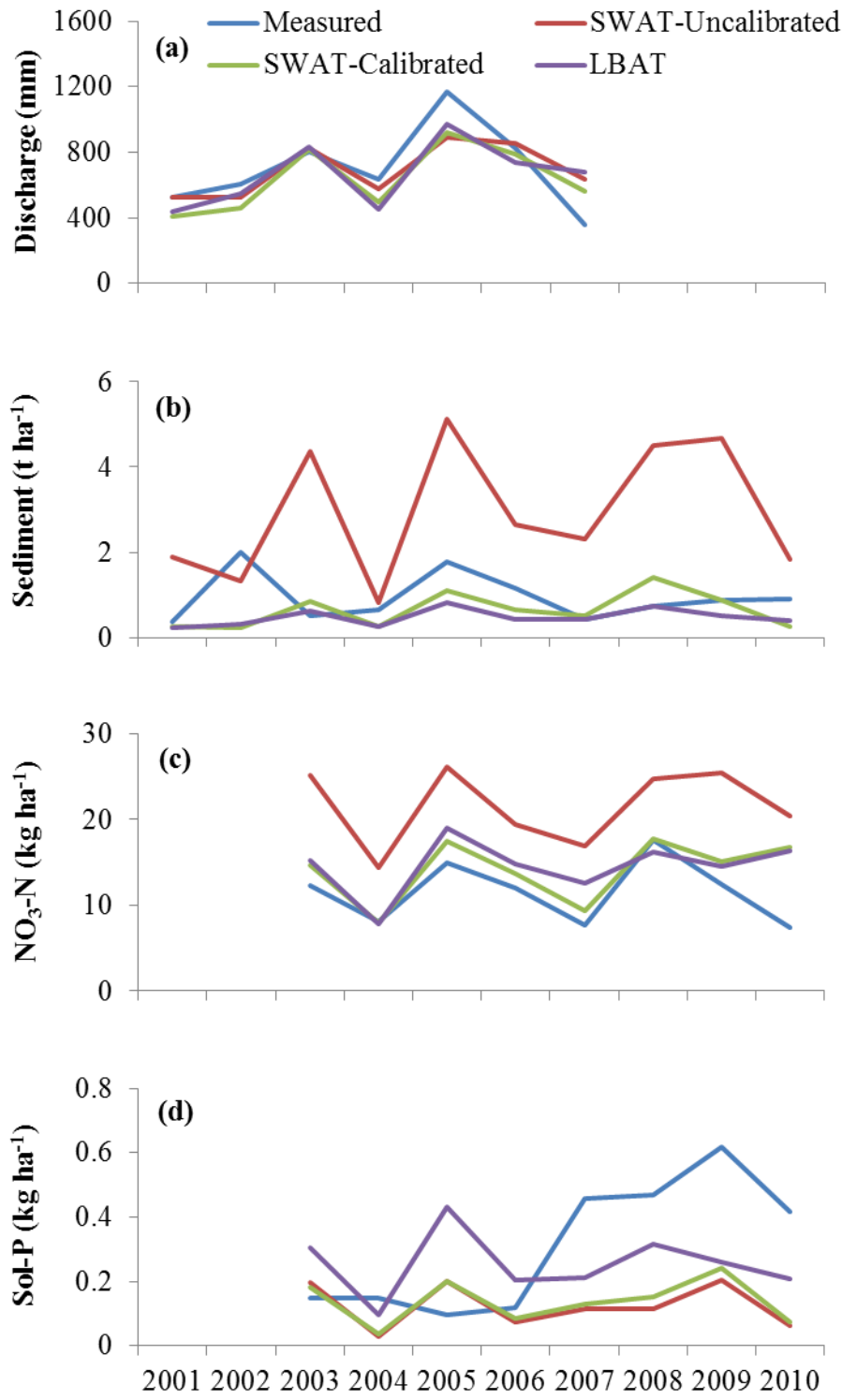
Period	Variable	Index	Measurement	SWAT -Uncalibrated	SWAT -Calibrated	LBAT ⁴⁵²
01-07	Discharge (mm)	Mean	704	691	638	453 4
		Re (%)	—	-2	-9	-6
		R ²	—	0.63	0.69	454 54
01-10	Sediment (t ha ⁻¹)	Mean	0.95	2.95	0.65	0.45
		Re (%)	—	212	-32	455 52
		R ²	—	0.01	0.01	456 0.04
03-10	NO ₃ -N (kg ha ⁻¹)	Mean	12	22	14	15
		Re (%)	—	87	22	457 37
		R ²	—	0.59	0.45	0.35
03-10	Sol-P (kg ha ⁻¹)	Mean	0.31	0.13	0.14	458 58
		Re (%)	—	-59	-55	-16
		R ²	—	0.02	0.11	459 59

460

461

462

463 Since LBAT is based on decision rules (statistical equations in this study) which
464 were derived from SWAT simulations for BBW, its usage should be constrained to areas
465 with soil, landscape, and land use characteristics similar to BBW. Input characteristics
466 exceeding the range of SWAT data could lead to large errors in predictions. LBAT is
467 flexible in its structure, and with thoughtful development of decision rules, it can be
468 applied to diverse environments.



469

470 **Fig. 5** Simulations of annual stream discharge and sediment, $\text{NO}_3\text{-N}$, and Sol-P loadings
 471 with LBAT and SWAT compared with field measurements at the outlet of LRW.

472

473 **3.2.3 FDT Assessment in LRW**

474 Mean annual water quantity and quality simulated with LBAT for agricultural lands of
475 LRW are shown in Table 8. The mean annual discharge for the baseline scenario was 626
476 mm greater than that for the six FDT scenarios (Table 8). When all agricultural lands
477 were protected (S6), there was a 2% reduction in discharge (equivalent to 11 mm; Table
478 8). With the steepest areas protected (accounting for 10% of the total land base; S1), the
479 mean annual sediment loading was reduced by as much as 43% (equivalent to 4.5 t ha⁻¹;
480 Table 8) and by as much as 81% (i.e., 8.57 t ha⁻¹) with all agricultural lands protected (S6;
481 Table 8). Mean annual Sol-P loading was reduced by 51% (equivalent to 0.47 kg ha⁻¹;
482 Table 8). In contrast, increased usage of FDT tended to increase the mean annual loading
483 of NO₃-N, by about 6% when used across all agricultural lands (equivalent to 1.73 kg ha⁻¹
484).

485

486

487

488

489

490

491

492

493

494 **Table 8** Impact of FDT on mean annual discharge and sediment, NO₃-N, and Sol-P
 495 loadings simulated with LBAT under different FDT, provided in Table 3.

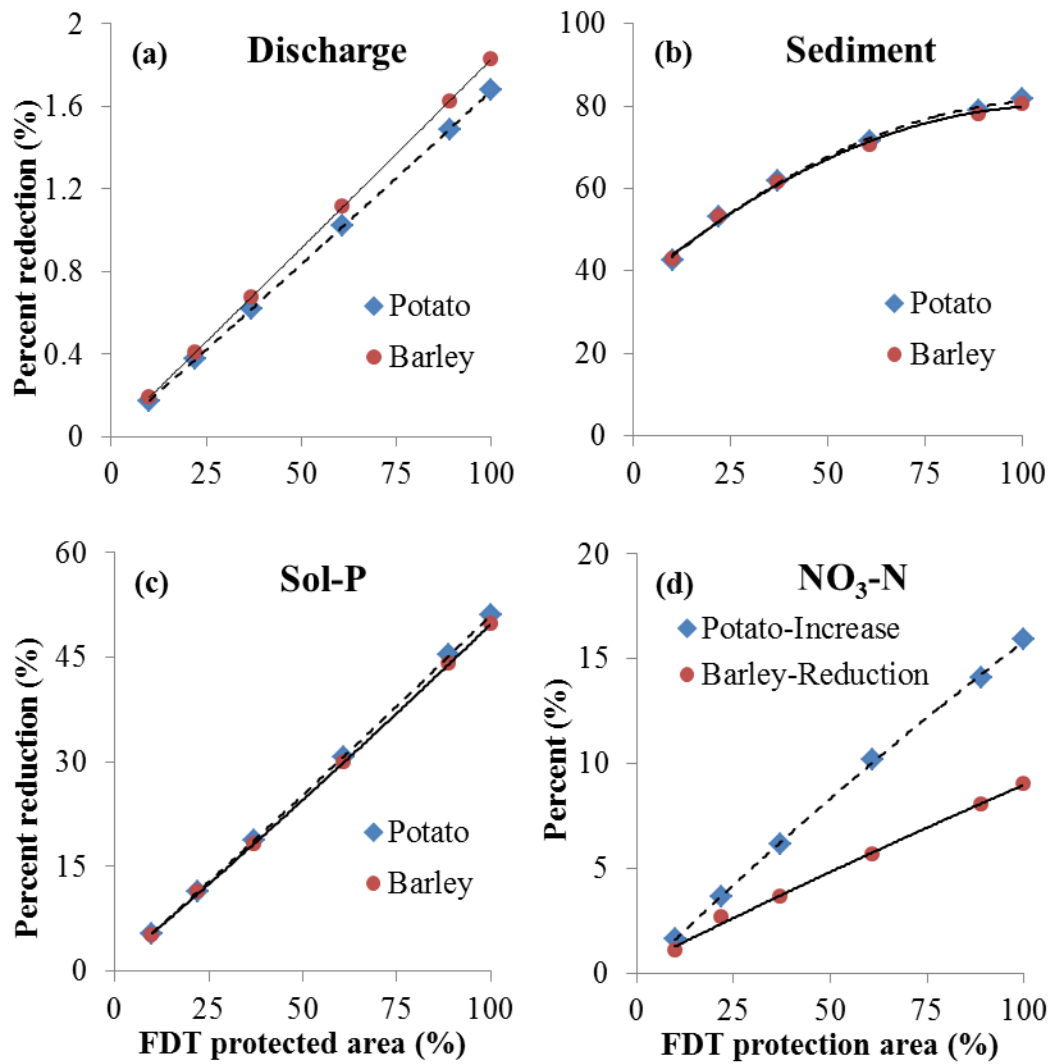
Variable	Index	Baseline	S1	S2	S3	S4	S5	S6
Discharge (mm)	Mean	626	625	623	622	619	616	615
	MD	—	-1	-2	-4	-7	-10	-11
	PRD (%)	—	0	0	-1	-1	-2	-2
Sediment (t ha ⁻¹)	Mean	10.54	6.04	4.94	4.02	3.04	2.26	1.97
	MD	—	-4.50	-5.60	-6.52	-7.50	-8.28	-8.57
	PRD (%)	—	-43	-53	-62	-71	-79	-81
NO ₃ -N (kg ha ⁻¹)	Mean	29.70	29.86	30.02	30.34	30.82	31.22	31.42
	MD	—	0.16	0.32	0.64	1.13	1.52	1.73
	PRD (%)	—	1	1	2	4	5	6
Sol-P (kg ha ⁻¹)	Mean	0.94	0.89	0.83	0.76	0.65	0.52	0.46
	MD	—	-0.05	-0.11	-0.17	-0.28	-0.42	-0.47
	PRD (%)	—	-5	-11	-19	-30	-45	-51

496

497 Percentage change (based on PRD) of water quantity and quality were plotted against
 498 percentage area of FDT for potato and barley in Fig. 6. Increasing the usage of FDT
 499 helped to reduce discharge and sediment and Sol-P loadings for both crop types (Figs. 6a,
 500 b, and c). It is worth noting that sediment loading decreased with increasing usage of
 501 FDT (Fig. 6b). An opposite trend was observed for potato and barley with respect to the
 502 impact of FDT on NO₃-N loading. With the increased usage of FDT, NO₃-N loadings
 503 increased linearly for potato, while it decreased for barley. The increased for potato was
 504 nearly twice as much as the reduction for barley (Fig. 6d). Seemingly the interaction
 505 between barley and FDT had positive impacts on nitrate retention in soils, whereas the
 506 interaction between potato and FDT had an opposite effect.

507 These results are consistent with the results from previous studies (Yang et al.,
 508 2012; Yang et al., 2010), which used SWAT to assess the impact of FDT on water
 509 quantity and quality within BBW. When using SWAT, greater efforts are needed to

510 prepare basic inputs, such as daily weather records, to proceed with its calibration and
 511 validation, involving complex scenario setup and analysis. For every new watershed,
 512 SWAT needs dedicated effort and time for its setup. LBAT, in contrast, can be used for
 513 multiple watersheds as long as they have similar environmental conditions. Scenario
 514 analysis can be directly conducted with different combinations of land use and BMPs
 515 using fewer inputs than what is required by SWAT. Also, once developed, LBAT does
 516 not require additional calibration.



517
 518 **Fig. 6** Percentage change in discharge and sediment, NO₃-N, and Sol-P loadings as a
 519 function of % area, where FDT's were used.

520 **4. Conclusion**

521 The present study addresses the development of a decision support tool to assess the
522 impact of land use change and BMPs on water quantity and quality for ungauged
523 watersheds. An enhanced version of SWAT was calibrated and validated for an small
524 experimental watershed. Multiple regression analyses were used to develop statistical
525 equations based on simulations from SWAT. In total, three discharge and five sediment,
526 $\text{NO}_3\text{-N}$, and Sol-P loading models were developed for different combinations of land use
527 groups and BMP scenarios. Only four common predictors (i.e., annual precipitation,
528 annual mean air temperature, mean saturated hydraulic conductivity of soil, and land use
529 groups) and three unique predictors (LS-factor and annual nitrogen and phosphorus
530 application rates for sediment, $\text{NO}_3\text{-N}$, and Sol-P loading models, respectively) are
531 required.

532 With the aid of ArcGIS, statistical equations were integrated into the decision support
533 tool, i.e., the land use and BMPs assessment tool (LBAT), whose basic simulation units
534 are the DEM-grid cell. The LBAT was used to simulate annual water flow and sediment
535 and nutrient loadings at the outlet of a larger watershed, i.e., Little River Watershed
536 (LRW). These simulations were compared with those of SWAT. Results indicated that
537 LBAT and the calibrated version of SWAT performed equivalently with respect to annual
538 stream discharge and sediment and $\text{NO}_3\text{-N}$ loadings. LBAT performed slightly better,
539 when Sol-P loading was considered. Compared with the uncalibrated version of SWAT,
540 LBAT performed better. The impact of FDT on water quantity and quality was evaluated
541 with LBAT for LRW; its results were consistent with the results generated with SWAT
542 for the same region in previous studies. LBAT has fewer input requirements than SWAT,

543 and can be applied to multiple watersheds without additional calibration. Also, scenario
544 analyses can be directly conducted with LBAT without complex setup procedures. We
545 recommend using LBAT for economic analysis and management decision making for
546 watersheds with similar environmental conditions of New Brunswick. The LBAT
547 developed in this study may not be directly applied to other regions; however, the
548 approach in developing LBAT can be applied to other regions of the world because of its
549 flexible structure.

550

551 **Acknowledgement**

552 The funding support for this project was provided by Agriculture and Agri-Food Canada
553 (AAFC) through project #1145, entitled “Integrating selected BMPs to maximize
554 environmental and economic benefits at the field and watershed scales for sustainable
555 potato production in New Brunswick”, and Natural Science and Engineering Research
556 Council (NSERC) through Discovery Grants to both CPAB and FRM. The research is
557 also partially supported by NASA (NNX17AE66G) and USDA (2017-67003-26485).
558 Authors are thankful to S. Lavoie, J. Monteith, and L. Stevens for their technical support
559 in data collection and sample analyses.

560

561

562

563

564

565

566 **Appendix A**567 **Table A1** Coefficient values for the three discharge models.

Model variable	Estimate	Std. Error	t-value	p-value
Dis1				
Intercept	-1565	24.04	-65.089	<0.001
PCP	1.933	0.02176	88.837	<0.001
TMP	282.7	6.091	46.402	<0.001
SOL_K	0.06338	0.00992	6.389	<0.001
FORT	30.79	14.16	2.175	0.030
NOCR	162.2	14.51	11.181	<0.001
PCP:TMP	-0.2488	0.005487	-45.352	<0.001
PCP:FORT	0.04684	0.01191	3.934	<0.001
PCP:NOCR	-0.0535	0.01224	-4.37	<0.001
TMP:FORT	9.723	1.684	5.775	<0.001
TMP:NOCR	4.506	1.731	2.603	0.009
SOL_K:FORT	-0.3769	0.03403	-11.076	<0.001
SOL_K:NOCR	-0.2959	0.032	-9.248	<0.001
Dis2				
Intercept	-1633	27.29	-59.84	<0.001
PCP	1.995	0.02472	80.69	<0.001
TMP	302.2	6.87	43.98	<0.001
SOL_K	0.08696	0.01167	7.45	<0.001
PCP:TMP	-0.2662	0.006199	-42.94	<0.001
Dis3				
Intercept	-1666	36.58	-45.54	<0.001
PCP	2.007	0.03305	60.713	<0.001
TMP	298	9.351	31.865	<0.001
SOL_K	0.09353	0.01573	5.946	<0.001
PCP:TMP	-0.2606	0.008406	-31.004	<0.001

568

569

570

571

572

573

574

Table A2 Coefficient values for the four sediment loading models.

Model variable	Estimate	Std. Error	t-value	p-value
Sed1_1				
Intercept	0.2749	0.06125	4.488	<0.001
USLE_LS	0.1201	0.02224	54.018	<0.001
PCP	0.000788	5.54E-05	14.218	<0.001
TMP	0.1117	0.01528	7.307	<0.001
SOL_K	0.000568	0.00022	2.585	0.010
GRAS	-0.0353	0.00881	-4.007	<0.001
USLE_LS:SOL_K	-0.00014	4.69E-05	-3.045	0.002
USLE_LS:GRAS	-0.02623	0.006826	-3.842	<0.001
PCP:TMP	-0.00011	1.38E-05	-7.967	<0.001
PCP:SOL_K	-4.6E-07	1.91E-07	-2.406	0.016
Sed1_2				
Intercept	0.8575	0.008826	97.15	<0.001
PCP	0.000123	7.82E-06	15.67	<0.001
PCP:USLE_LS	0.000209	5.02E-06	41.65	<0.001
Sed1_3				
(Intercept)	0.3992	0.02267	17.613	<0.001
USLE_LS	0.07935	0.01967	4.034	<0.001
PCP	0.000204	1.96E-05	10.371	<0.001
SOL_K	0.000545	5.71E-05	9.534	<0.001
USLE_LS:PCP	4.94E-05	1.71E-05	2.9	0.004
USLE_LS:SOL_K	-0.00067	4.89E-05	-13.718	<0.001
Sed2				
Intercept	0.2591	0.05228	4.956	<0.001
USLE_LS	0.12	0.001898	63.218	<0.001
PCP	0.000767	4.73E-05	16.212	<0.001
TMP	0.1162	0.01304	8.907	<0.001
SOL_K	0.000746	0.000188	3.981	<0.001
GRAS	-0.06937	0.01648	-4.211	<0.001
USLE_LS:SOL_K	-0.00013	4E-05	-3.137	0.002
USLE_LS:GRAS	-0.02662	0.005829	-4.567	<0.001
PCP:TMP	-0.00011	1.18E-05	-9.522	<0.001
PCP:SOL_K	-6.3E-07	1.63E-07	-3.846	<0.001
TMP:GRAS	0.007415	0.003664	2.024	0.043

579 **Table A3** Coefficient values for the four $\text{NO}_3\text{-N}$ loading models corresponding to land
 580 use and BMPs described in Table 4.

Model variable	Estimate	Std. Error	t-value	p-value
N1_1				
Intercept	1.44	0.1753	8.213	<0.001
N_APP	-0.00862	0.000699	-12.325	<0.001
PCP	0.000543	0.00016	3.4	<0.001
TMP	0.1363	0.03357	4.059	<0.001
SOL_K	-0.00344	9.78E-05	-35.163	<0.001
GRAN	-1.117	0.1021	-10.937	<0.001
GRAS	-1.97	0.1562	-12.611	<0.001
N_APP:PCP	5.31E-06	6.45E-07	8.233	<0.001
N_APP:TMP	0.000963	7.45E-05	12.929	<0.001
N_APP:SOL_K	9.6E-06	6.4E-07	15.024	<0.001
PCP:GRAN	0.000677	9.38E-05	7.215	<0.001
PCP:GRAS	0.001029	0.000143	7.201	<0.001
PCP:TMP	-0.00025	2.64E-05	-9.467	<0.001
TMP:GRAN	0.1	0.01134	8.817	<0.001
TMP:GRAS	0.2132	0.01651	12.912	<0.001
N1_3				
Intercept	-1.411	0.3087	-4.573	<0.001
PCP	0.001875	0.000279	6.710	<0.001
TMP	0.4437	0.07831	5.666	<0.001
SOL_K	-0.00104	0.000116	-8.979	<0.001
PCP:TMP	-0.00032	7.06E-05	-4.484	<0.001
N2				
Intercept	1.429	0.1757	8.134	<0.001
N_APP	-0.00858	0.000701	-12.233	<0.001
PCP	0.000548	0.00016	3.425	<0.001
TMP	0.1376	0.03365	4.089	<0.001
SOL_K	-0.00345	9.8E-05	-35.223	<0.001
GRAN	-1.11	0.1023	-10.849	<0.001
GRAS	-1.962	0.1566	-12.526	<0.001
N_APP:PCP	5.3E-06	6.47E-07	8.187	<0.001
N_APP:TMP	0.000957	7.46E-05	12.82	<0.001
N_APP:SOL_K	9.65E-06	6.4E-07	15.067	<0.001
PCP:GRAN	0.000674	9.41E-05	7.167	<0.001
PCP:GRAS	0.001026	0.000143	7.162	<0.001
PCP:TMP	-0.00025	2.64E-05	-9.456	<0.001
TMP:GRAN	0.09934	0.01137	8.738	<0.001
TMP:GRAS	0.2122	0.01655	12.821	<0.001

N3				
Intercept	-0.3595	0.1718	-2.092	0.037
N_APP	-0.00131	0.000435	-3.011	0.003
PCP	0.001621	0.00015	10.806	<0.001
TMP	0.3977	0.03857	10.312	<0.001
SOL_K	-0.00386	0.000505	-7.641	<0.001
GRAN	-0.2133	0.07504	-2.842	0.005
N_APP:PCP	1.65E-06	3.59E-07	4.61	<0.001
N_APP:TMP	0.000281	4.74E-05	5.939	<0.001
N_APP:GRAN	0.000716	0.000292	2.453	0.014
PCP:TMP	-0.00035	3.32E-05	-10.506	<0.001
PCP:SOL_K	1.21E-06	4.36E-07	2.781	0.005
PCP:GRAN	0.000267	5.82E-05	4.577	<0.001
TMP:GRAN	-0.04685	0.008004	-5.853	<0.001

581

582

583

584

585

586

587

588

589

590

591

592

593

594

595

596

Table A4 Coefficient values for four Sol-P models.

Model variable	Estimate	Std. Error	t-value	p-value
P1_1				
Intercept	-3.711	0.1306	-28.416	<0.001
P_APP	0.002341	0.000623	3.757	<0.001
PCP	0.003195	0.000117	27.286	<0.001
TMP	0.5542	0.03197	17.337	<0.001
SOL_K	0.00298	0.000472	6.305	<0.001
GRAS	-0.4321	0.0382	-11.312	<0.001
P_APP:PCP	-2.4E-06	5.2E-07	-4.64	<0.001
P_APP:TMP	0.000829	7.7E-05	10.797	<0.001
PCP:TMP	-0.00052	2.9E-05	-18.297	<0.001
PCP:SOL_K	-1.2E-06	3. 97E-07	-3.095	0.002
TMP:SOL_K	-0.00026	5.7E-05	-4.526	<0.001
TMP:GRAS	0.03787	0.00941	4.024	<0.001
P1_3				
Intercept	-4.43817	0.589848	-7.512	<0.001
PCP	0.002509	0.000534	4.701	<0.001
TMP	0.417306	0.1496445	2.789	0.005
SOL_K	0.001247	0.000222	5.622	<0.001
PCP:TMP	-0.0003	0.000135	-2.253	0.024
P2				
Intercept	-3.667	0.1357	-27.017	<0.001
P_APP	0.003461	0.000663	5.218	<0.001
PCP	0.003017	0.000122	24.783	<0.001
TMP	0.5149	0.03304	15.584	<0.001
SOL_K	0.003531	0.000488	7.233	<0.001
GRAS	-0.2039	0.09001	-2.265	0.024
P_APP:PCP	-2.4E-06	5.54E-07	-4.305	<0.001
P_APP:TMP	0.000432	7.93E-05	5.445	<0.001
P_APP:GRAS	-0.03304	0.007019	-4.707	<0.001
PCP:TMP	-0.00044	2.95E-05	-14.952	<0.001
PCP:SOL_K	-1.4E-06	4.1E-07	-3.446	<0.001
PCP:GRAS	-0.00025	7.66E-05	-3.25	0.001
TMP:SOL_K	-0.00025	5.87E-05	-4.184	<0.001
TMP:GRAS	0.05117	0.009839	5.201	<0.001
P3				
Intercept	-2.817	0.2548	-11.054	<0.001
P_APP	-0.01363	0.001854	-7.352	<0.001
PCP	0.002778	0.000178	15.609	<0.001
TMP	0.1406	0.06523	2.155	0.031
SOL_K	0.00651	0.000702	9.279	<0.001

GRAN	-0.9386	0.1378	-6.812	<0.001
GRAS	-0.9931	0.1813	-5.478	<0.001
P_APP:TMP	0.003562	0.000491	7.252	<0.001
P_APP:GRAN	0.007736	0.002179	3.549	<0.001
P_APP:GRAS	-0.05489	0.01295	-4.24	<0.001
PCP:TMP	-0.0003	4.42E-05	-6.763	<0.001
PCP:SOL_K	-3.7E-06	5.78E-07	-6.359	<0.001
PCP:GRAN	0.000112	5.1E-05	2.192	0.028
PCP:GRAS	-0.00019	0.000109	-1.74	0.082
TMP:SOL_K	-0.00021	8.8E-05	-2.4	0.016
TMP:GRAN	0.1798	0.03332	5.397	<0.001
TMP:GRAS	0.247	0.03581	6.898	<0.001

598

599

600

601 **References**

602

603 Arnold, J. G., Srinivasan, R., Muttiah, R. S., and Williams, J. R.: Large area hydrologic
604 modeling and assessment part I: Model development, JAWRA Journal of the
605 American Water Resources Association, 34, 73-89, 1998.

606 Beasley, D., Huggins, L., and Monke, a.: ANSWERS: A model for watershed planning,
607 Transactions of the ASAE, 23, 938-0944, 1980.

608 Beaulac, M. N., and Reckhow, K. H.: An Examination of Land Use - Nutrient Export
609 Relationships, JAWRA Journal of the American Water Resources Association, 18,
610 1013-1024, 1982.

611 Blöschl, G., and Sivapalan, M.: Scale issues in hydrological modelling: a review,
612 Hydrological processes, 9, 251-290, 1995.

613 Bloschl, G., and Grayson, R.: Spatial observations and interpolation, Spatial patterns in
614 catchment hydrology: observations and modelling, edited by: Grayson, R. and
615 Bloschl, G., Cambridge University Press, UK, ISBN 0-521-63316-8, 17-50, 2001.

616 Borah, D., and Bera, M.: Watershed-scale hydrologic and nonpoint-source pollution
617 models: Review of mathematical bases, *Transactions of the ASAE*, 46, 1553, 2003.

618 Borah, D. K., Demissie, M., and Keefer, L. L.: AGNPS-based assessment of the impact
619 of BMPs on nitrate-nitrogen discharging into an Illinois water supply lake, *Water*
620 *International*, 27, 255-265, 2002.

621 Borah, D. K., and Bera, M.: Watershed-scale hydrologic and nonpoint-source pollution
622 models: Review of applications, *Transactions of the ASAE*, 47, 789-803, 2004.

623 Chow, L., Xing, Z., Benoy, G., Rees, H., Meng, F., Jiang, Y., and Daigle, J.: Hydrology
624 and water quality across gradients of agricultural intensity in the Little River
625 watershed area, New Brunswick, Canada, *Journal of Soil and Water Conservation*,
626 66, 71-84, 2011.

627 Chow, T., and Rees, H.: Impacts of intensive potato production on water yield and
628 sediment load (Black Brook Experimental Watershed: 1992–2002 summary), Potato
629 Research Centre, AAFC, Fredericton, 26, 2006.

630 D'Arcy, B., and Frost, A.: The role of best management practices in alleviating water
631 quality problems associated with diffuse pollution, *Science of the Total*
632 *Environment*, 265, 359-367, 2001.

633 Endreny, T. A., and Wood, E. F.: WATERSHED WEIGHTING OF EXPORT
634 COEFFICIENTS TO MAP CRITICAL PHOSPHOROUS LOADING AREAS1, in,
635 Wiley Online Library, 2003.

636 Ihaka, R., and Gentleman, R.: R: a language for data analysis and graphics, *Journal of*
637 *computational and graphical statistics*, 5, 299-314, 1996.

638 Keselman, H., Huberty, C. J., Lix, L. M., Olejnik, S., Cribbie, R. A., Donahue, B.,
639 Kowalchuk, R. K., Lowman, L. L., Petoskey, M. D., and Keselman, J. C.: Statistical
640 practices of educational researchers: An analysis of their ANOVA, MANOVA, and
641 ANCOVA analyses, *Review of Educational Research*, 68, 350-386, 1998.

642 Knisel, W. G.: CREAMS: a field scale model for Chemicals, Runoff, and Erosion from
643 Agricultural Management Systems [USA], United States. Dept. of Agriculture.
644 Conservation research report (USA), 1980.

645 Leonard, R., Knisel, W., and Still, D.: GLEAMS: Groundwater loading effects of
646 agricultural management systems, *Transactions of the ASAE*, 30, 1403-1418, 1987.

647 Li, Q., Qi, J., Xing, Z., Li, S., Jiang, Y., Danielescu, S., Zhu, H., Wei, X., and Meng, F.-
648 R.: An approach for assessing impact of land use and biophysical conditions across
649 landscape on recharge rate and nitrogen loading of groundwater, *Agriculture,
650 Ecosystems & Environment*, 196, 114-124, 10.1016/j.agee.2014.06.028, 2014.

651 Liu, Y., Yang, W., Yu, Z., Lung, I., and Gharabaghi, B.: Estimating sediment yield from
652 upland and channel erosion at a watershed scale using SWAT, *Water Resources
653 Management*, 29, 1399-1412, 2015.

654 Marshall, I., Schut, P., and Ballard, M.: A national ecological framework for Canada:
655 Attribute data. Ottawa, Ontario: Environmental Quality Branch, Ecosystems Science
656 Directorate, Environment Canada and Research Branch, Agriculture and Agri-Food
657 Canada, 1999.

658 May, L., and Place, C.: A GIS-based model of soil erosion and transport, *Freshwater
659 Forum*, 2010,

660 Mellerowicz, K. T.: Soils of the Black Brook Watershed St. Andre Parish, Madawaska
661 County, New Brunswick, [Fredericton]: New Brunswick Department of Agriculture,
662 1993.

663 Mostaghimi, S., Park, S., Cooke, R., and Wang, S.: Assessment of management
664 alternatives on a small agricultural watershed, *Water Research*, 31, 1867-1878, 1997.

665 Novara, A., Gristina, L., Saladino, S., Santoro, A., and Cerdà, A.: Soil erosion assessment
666 on tillage and alternative soil managements in a Sicilian vineyard, *Soil and Tillage
667 Research*, 117, 140-147, 2011.

668 Ongley, E. D., Xiaolan, Z., and Tao, Y.: Current status of agricultural and rural non-point
669 source pollution assessment in China, *Environmental Pollution*, 158, 1159-1168,
670 2010.

671 Panagopoulos, Y., Makropoulos, C., and Mimikou, M.: Reducing surface water pollution
672 through the assessment of the cost-effectiveness of BMPs at different spatial scales,
673 *Journal of environmental management*, 92, 2823-2835, 2011.

674 Pimentel, D., and Krummel, J.: Biomass energy and soil erosion: Assessment of resource
675 costs, *Biomass*, 14, 15-38, 1987.

676 Qi, J., Li, S., Li, Q., Xing, Z., Bourque, C. P.-A., and Meng, F.-R.: A new soil-
677 temperature module for SWAT application in regions with seasonal snow cover,
678 *Journal of Hydrology*, 538, 863-877, 2016a.

679 Qi, J., Li, S., Li, Q., Xing, Z., Bourque, C. P.-A., and Meng, F.-R.: Assessing an
680 Enhanced Version of SWAT on Water Quantity and Quality Simulation in Regions
681 with Seasonal Snow Cover, *Water Resources Management*, 1-17, 2016b.

682 Qi, J., Li, S., Jamieson, R., Hebb, D., Xing, Z., and Meng, F.-R.: Modifying SWAT with
683 an energy balance module to simulate snowmelt for maritime regions,
684 Environmental Modelling & Software, 93, 146-160, 2017a.

685 Qi, J., Li, S., Yang, Q., Xing, Z., and Meng, F.-R.: SWAT Setup with Long-Term
686 Detailed Landuse and Management Records and Modification for a Micro-
687 Watershed Influenced by Freeze-Thaw Cycles, Water Resources Management, 31,
688 3953-3974, 10.1007/s11269-017-1718-2, 2017b.

689 Quan, W., and Yan, L.: Effects of agricultural non-point source pollution on eutrophica-
690 tion of water body and its control measure, Acta Ecologica Sinica, 22, 291-299,
691 2001.

692 Reckhow, K., and Simpson, J.: A procedure using modeling and error analysis for the
693 prediction of lake phosphorus concentration from land use information, Canadian
694 Journal of Fisheries and Aquatic Sciences, 37, 1439-1448, 1980.

695 Renschler, C., and Lee, T.: Spatially distributed assessment of short-and long-term
696 impacts of multiple best management practices in agricultural watersheds, Journal of
697 Soil and Water Conservation, 60, 446-456, 2005.

698 Renschler, C. S., and Harbor, J.: Soil erosion assessment tools from point to regional
699 scales—the role of geomorphologists in land management research and
700 implementation, Geomorphology, 47, 189-209, 2002.

701 Sadeghi, S. H., Moosavi, V., Karami, A., and Behnia, N.: Soil erosion assessment and
702 prioritization of affecting factors at plot scale using the Taguchi method, Journal of
703 hydrology, 448, 174-180, 2012.

704 Sharpley, A. N., and Williams, J. R.: EPIC-erosion/productivity impact calculator: 1.
705 Model documentation, Technical Bulletin-United States Department of Agriculture,
706 1990.

707 Singh, V. P.: Computer models of watershed hydrology, Water Resources Publications,
708 1995.

709 Singh, V. P., and Woolhiser, D. A.: Mathematical modeling of watershed hydrology,
710 Journal of hydrologic engineering, 7, 270-292, 2002.

711 Singh, V. P., and Frevert, D. K.: Watershed Models, CRC Press, Boca Raton, FL, USA,
712 2005.

713 Turkelboom, F., Poesen, J., Ohler, I., Van Keer, K., Ongprasert, S., and Vlassak, K.:
714 Assessment of tillage erosion rates on steep slopes in northern Thailand, Catena, 29,
715 29-44, 1997.

716 Urbonas, B.: Assessment of stormwater BMPs and their technology, Water Science and
717 Technology, 29, 347-353, 1994.

718 Vörösmarty, C. J., McIntyre, P. B., Gessner, M. O., Dudgeon, D., Prusevich, A., Green,
719 P., Glidden, S., Bunn, S. E., Sullivan, C. A., and Liermann, C. R.: Global threats to
720 human water security and river biodiversity, Nature, 467, 555-561, 2010.

721 Vanoni, V. A.: Sedimentation Engineering: American Society of Civil Engineers,
722 Manuals and Reports on Engineering Practice, 1975.

723 Veldkamp, A., and Lambin, E. F.: Predicting land-use change, Agriculture, ecosystems &
724 environment, 85, 1-6, 2001.

725 Viavattene, C., Scholes, L., Revitt, D., and Ellis, J.: A GIS based decision support system
726 for the implementation of stormwater best management practices, 11th International
727 Conference on Urban Drainage, Edinburgh, Scotland, UK, 2008,

728 Wilson, C. J., Carey, J. W., Beeson, P. C., Gard, M. O., and Lane, L. J.: A GIS - based
729 hillslope erosion and sediment delivery model and its application in the Cerro
730 Grande burn area, *Hydrological Processes*, 15, 2995-3010, 2001.

731 Xing, Z., Chow, L., Rees, H., Meng, F., Li, S., Ernst, B., Benoy, G., Zha, T., and Hewitt,
732 L. M.: Influences of sampling methodologies on pesticide-residue detection in
733 stream water, *Archives of environmental contamination and toxicology*, 64, 208-218,
734 2013.

735 Yang, Q., Meng, F.-R., Zhao, Z., Chow, T. L., Benoy, G., Rees, H. W., and Bourque, C.
736 P.-A.: Assessing the impacts of flow diversion terraces on stream water and
737 sediment yields at a watershed level using SWAT model, *Agriculture, ecosystems &*
738 *environment*, 132, 23-31, 2009.

739 Yang, Q., Zhao, Z., Benoy, G., Chow, T. L., Rees, H. W., Bourque, C. P.-A., and Meng,
740 F.-R.: A watershed-scale assessment of cost-effectiveness of sediment abatement
741 with flow diversion terraces, *Journal of environmental quality*, 39, 220-227, 2010.

742 Yang, Q., Benoy, G. A., Chow, T. L., Daigle, J.-L., Bourque, C. P.-A., and Meng, F.-R.:
743 Using the Soil and Water Assessment Tool to estimate achievable water quality
744 targets through implementation of beneficial management practices in an
745 agricultural watershed, *Journal of environmental quality*, 41, 64-72, 2012.

746 Young, R. A., Onstad, C., Bosch, D., and Anderson, W.: AGNPS: A nonpoint-source
747 pollution model for evaluating agricultural watersheds, *Journal of soil and water
748 conservation*, 44, 168-173, 1989.

749 Zhang, W., Wu, S., Ji, H., and Kolbe, H.: Estimation of agricultural non-point source
750 pollution in China and the alleviating strategies I. Estimation of agricultural non-
751 point source pollution in China in early 21 century, *Scientia agricultura sinica*, 37,
752 1008-1017, 2004.

753 Zhao, Z., Chow, T. L., Yang, Q., Rees, H. W., Benoy, G., Xing, Z., and Meng, F.-R.:
754 Model prediction of soil drainage classes based on digital elevation model
755 parameters and soil attributes from coarse resolution soil maps, *Canadian Journal of
756 Soil Science*, 88, 787-799, 2008.

757 Zhao, Z., Benoy, G., Chow, T. L., Rees, H. W., Daigle, J.-L., and Meng, F.-R.: Impacts
758 of accuracy and resolution of conventional and LiDAR based DEMs on parameters
759 used in hydrologic modeling, *Water resources management*, 24, 1363-1380, 2010.

760